European Journal of Medicinal Chemistry 103 (2015) 409–417

Contents lists available at ScienceDirect

European Journal of Medicinal Chemistry

journal homepage: http://www.elsevier.com/locate/ejmech

Research paper

Novel 3,4-methylenedioxyde-6-X-benzaldehyde-thiosemicarbazones: Synthesis and antileishmanial effects against *Leishmania amazonensis*

Jorge Luiz R. de Melos [a], Eduardo Caio Torres-Santos [b], Viviane dos S. Faiões [b], Catarina de Nigris Del Cistia [a], Carlos Maurício R. Sant'Anna [a], Cláudio Eduardo Rodrigues-Santos [a], Aurea Echevarria [a, *]

[a] Departamento de Química, Universidade Federal Rural do Rio de Janeiro, 23.890-000 Seropédica, RJ, Brazil
[b] Laboratório de Bioquímica de Tripanosomatídeos, Instituto Oswaldo Cruz, FIOCRUZ, Rio de Janeiro, Brazil

ARTICLE INFO

Article history:
Received 16 March 2015
Received in revised form
2 July 2015
Accepted 5 September 2015
Available online 8 September 2015

Keywords:
Leishmania amazonensis
Promastigotes
Amastigotes
Thiosemicarbazones

ABSTRACT

A series of eleven 3,4-methylenedioxyde-6-X-benzaldehyde-thiosemicarbazones (**16**–**27**) was synthesised as part of a study to search for potential new drugs with a leishmanicidal effect. The thiosemicarbazones, ten of which are new compounds, were prepared in good yields (85–98%) by the reaction of 3,4-methylenedioxyde-6-benzaldehydes (6-X-piperonal), previously synthesised for this work by several methodologies, and thiosemicarbazide in ethanol with a few drops of H_2SO_4. These compounds were evaluated against *Leishmania amazonensis* promastigotes, and derivatives where X = I (**22**) and X = CN (**23**) moieties showed impressive results, having IC_{50} = 20.74 μM and 16.40 μM, respectively. The intracellular amastigotes assays showed IC_{50} = 22.00 μM (**22**) and 17.00 μM (**23**), and selectivity index >5.7 and >7.4, respectively, with a lower toxicity compared to pentamidine (positive control, SI = 4.5). The results obtained from the preliminary QSAR study indicated the hydrophobicity (log *P*) as a fundamental parameter for the 2D-QSAR linear model. A molecular docking study demonstrated that both compounds interact with flavin mononucleotide (FMN), important binding site of NO synthase.

1. Introduction

Leishmaniasis is a group of diseases caused by protozoan parasites of the *Leishmania* genus transmitted by infected sand-flies. These diseases can manifest in three forms depending on the parasite species and the immune system of the patient: cutaneous, mucocutaneous and visceral. This disease is endemic in several tropical and sub-tropical countries and has been recognised as an increasing public health problem by the World Health Organization (WHO) [1–3].

The first choice treatments for leishmaniasis involve the use of pentavalent antimonial derivatives (sodium stibogluconate and meglumine antimoniate) that are highly toxic with serious side effects and a prolonged treatment regimen [4]. Alternatives include pentamidine, paromomycin, amphotericin B and miltefosine, but these drugs have not found extensive use because of severe toxicities and difficulties with parenteral administration and drug resistance [5–8]. The search of new, safe and efficient antiparasitic agents for the treatment of leishmaniasis is an urgent need and a pressing concern for global health programs.

Thiosemicarbazones have remarkable biological activities, including anticancer [9,10], antibacterial [11,12], antiviral [13] and antiparasitic properties [14,15]. Recently, we reported the anti-*Trypanosoma cruzi* activity of some thiosemicarbazones that demonstrated a good trypanocidal effect [16,17]. Furthermore, a significant decrease in nitric oxide synthase enzyme activity was observed along with the absence of macrophage toxicity for any of the assayed compounds [16]. These results motivated us to prepare a new series of thiosemicarbazones containing 3,4-dimethylene dioxyde substituted moieties, an important chemical group found in several molecules with biological activity.

Thus, in an effort to obtain thiosemicarbazones with high leishmanicidal activity and low toxicity, we present the synthesis of eleven compounds, 3,4-methylenedioxyde-6-X-benzaldehyde-thiosemicarbazones (**16**–**27**), where X = H (**16**), NO_2 (**17**), NH_2 (**18**), F (**19**), Cl (**20**), Br (**21**), I (**22**), CN (**23**), OH (**24**), OCH_3 (**25**) and

* Corresponding author.
E-mail address: echevarr@ufrrj.br (A. Echevarria).

http://dx.doi.org/10.1016/j.ejmech.2015.09.009
0223-5234/

$NHCOCH_2Cl$ (**26**). The *in vitro* experiments using *Leishmania amazonensis* were carried out to ten compounds against cultured promastigotes. Furthermore, the effect of most active compounds was evaluated against amastigote-infected peritoneal mouse macrophages.

2. Results and discussion

2.1. Chemistry

2.1.1. Synthesis of 3,4-methylenedioxyde-6-X-benzaldehydes

A series of twelve 3,4-methylenedioxyde-6-X-benzaldehyde-thiosemicarbazones, including eleven new compounds, was prepared starting from 3,4-methylenedioxyde-6-X-benzaldehydes (6-X-piperonal). The preparation of aldehydes was carried out by several methodologies according to the electronic characteristics of specific moieties. Scheme 1 shows the methods used to prepare the eleven 3,4-methylenedioxyde-6-X-benzaldehydes. Only the piperonal (**1**) was commercially available. The aldehyde **2** was prepared by nitration with concentrated nitric acid as previously described [18] in 76% yield; **3** was obtained by treatment of **2** with $FeSO_4$ in the presence of ammonium [19] in 65% yield. Compounds **4** [20] and **5** [21] were obtained by treatment of the diazonium salt of **3** with HBF_4 and slowly stirred at room temperature under Sandmayer reaction conditions in 62% and 58% yields, respectively. The aldehyde **6** was obtained by reaction of **5** with dimethylsulphate in anhydrous benzene in 93% yield [22]. The aldehyde **7** was obtained by treatment of **3** with $ClCH_2COCl$ in 84% yield. Halogenated piperonals where X = Cl (**8**) or Br (**9**) were prepared directly from the piperonal using trichloroisocianuric acid in pyridine, as a Lewis base, and ethanol in 96% yield for **8** [23] and bromine in acetic acid and ethanol to afford **9** in 70% yield [24]. Compound **9** was protected with ethylene glycol and reacted with CuCN in anhydrous dimethylformamide [25], followed by an acidic hydrolysis to yield the aldehyde **10** in 67% yield. Finally, the aldehyde **13** was prepared by treating reduced piperonal (piperonol, **11**, by

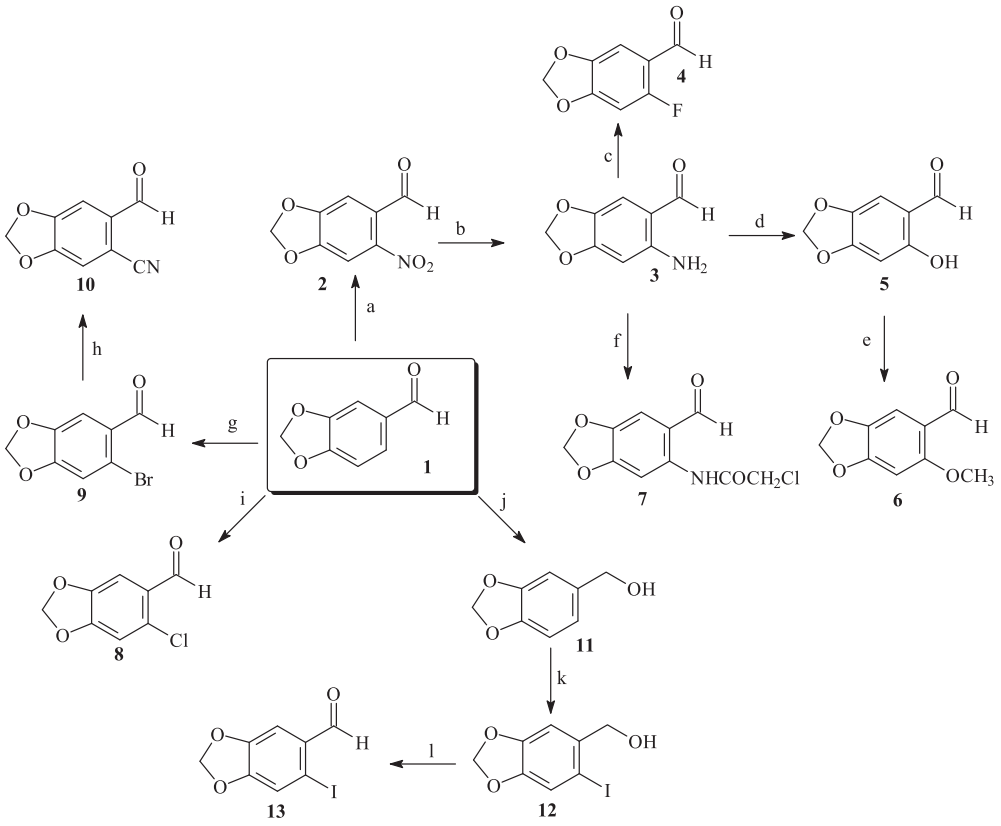

* a: HNO_3, rt, 30 min; b: $FeSO_4$ in hot H_2O, NH_4OH, 10 min; c: i) HCl, $NaNO_2$, H_2O, 5° C, ii) HBF_4 (48%), 60-70 °C, 8 h; d: i) H_2SO_4 drops, $NaNO_2$, H_2O, 5 °C, ii) $CuSO_4$, H_2O, 100° C, 8 h; e: anhydrous K_2CO_3, benzene, dimethylsulfphate, reflux, 48 h; f: anhydrous pyridine, chloroacetic anhydride, ether, 3 h; g: bromine, CH_3OH, acetic acid drops, rt, until complete consumption of piperonal, $NaHSO_4$, (1 mol.L^{-1}); h: i) $HOCH_2CH_2OH$, *p*-toluenesulphonic acid, toluene, reflux, 20 h, ii) CuCN, DMF, reflux, 3 h, iii) aq. HCl (5%), 50-60 °C, 15 min; i: trichlorocianuric acid, ethanol, 50 °C, 3 h; j: i) $NaBH_4$ (10%), MeOH, NaOH (0.05 mol.L^{-1}) rt, 50 min, ii) HCl (6 mol.L^{-1}); k: i) iodine, MeOH, $AgNO_3$, trifluoroacetic acid, rt, 2 h, ii) sodium thiosulphate; l: i) PCC, CH_2Cl_2, 50 °C, 40 min, ii) NaOH (1 mol.L^{-1}).

Scheme 1. Syntheses of 6-X-piperonal (**2**–**11** and **14**) and the intermediates **12** and **13**.

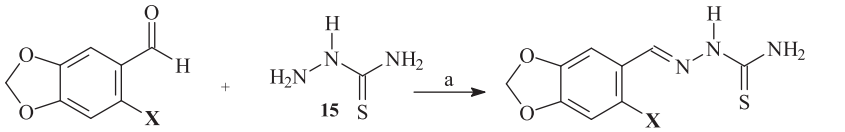

1 X = H; **2** X = NO_2; **3** X = NH_2; **4** X = F; **5** X = OH; **6** X = OCH_3; **7** X = $NHCOCH_2Cl$; **8** X = $NHCOCF_3$; **9** X = Cl; **10** X = Br; **11** X = CN; **14** X = I

16 X = H; **17** X = NO_2; **18** X = NH_2; **19** X = F; **20** X = Cl; **21** X = Br; **22** X = I; **23** X = CN; **24** X = OH; **25** X = OCH_3; **26** X = $NHCOCH_2Cl$

a: few drops H_2SO_4, ethanol, 40 °C, 4 h

Scheme 2. Synthesis of 6-X-piperonal thiosemicarbazones (**16**–**26**).

reaction with $NaBH_4$, 97%) with iodine in the presence of silver trifluoroacetate in methanol [26] to afford **12** in 97% yield. Compound **12** was subsequently submitted to an oxidation reaction with PCC (pyridinium chlorochromate) in dichloromethane [27] to afford the aldehyde **13** in 70% yield.

The aldehydes were characterised by routine spectroscopic techniques, which verified that the infrared absorption of the carbonyl group was in the range of 1652–1683 cm^{-1}, the values of the H–CO chemical shifts were between δ 9.57–10.20 and the values for the HCO shifts were between δ 188.6–194.5, in accordance with expected values. The shifts chemicals were registered by Bruker NMR 400 MHz or 500 MHz spectrometers (see Supplementary Data).

2.1.2. Synthesis of 3,4-methylenedioxyde-6-X-benzaldehyde-thiosemicarbazones

A series of twelve 3,4-methylenedioxyde-6-X-benzaldehyde-thiosemicarbazones (**16**–**26**), ten of which are described here for the first time, was prepared from the previously synthesised 3,4-methylenedioxyde-6-X-benzaldehydes (**1**–**11** and **14**) and thiosemicarbazide (**15**) using a few drops of H_2SO_4 and ethanol as solvent at 60 °C within 240 min (Scheme 2). The products were recrystallised from methanol in 85–98% yield.

The infrared spectra shows the disappearance of the carbonyl band at 1652 to 1683 cm^{-1}, and new ν (C=N) bands at 1541 and 1500 cm^{-1}, and a ν (C=S) band at 1043 to 1103 cm^{-1} resulting from the presence of thiosemicarbazone, as reported in the literature [28].

^1H and ^{13}C NMR spectra (supplementary data) permitted the full characterisation of all thiosemicarbazones. The ^1H NMR chemical shifts of the NH_2 group presented two distinct shifts, a hydrogen shift at downfield, probably due to an intramolecular hydrogen bond with the azomethine nitrogen, as characterized by theoretical and experimental data [29,30]. It was possible to observe on the ^{13}C NMR spectra chemical shifts at δ 177–179 and δ 139–149 corresponding to C=S and C=N, respectively, according to the literature [29,30] (see Supplementary Data). Furthermore, the doublet with chemical shifts centred at δ 158.3 with a coupling constant of 353 Hz confirmed the F–C6′ for compound **19**.

2.2. In vitro antileishmanial assays

2.2.1. Antileishmanial assays against L. amazonensis promastigotes

The treatment of the parasites with the thiosemicarbazones **16**–**24** and **26** resulted in the dose-dependent growth inhibition of *L. amazonensis* promastigotes. The 50% growth inhibitory activity value, IC_{50}, after 72 h of culture of each compound was assessed by the MTT assay [31], and the values were determined by linear regression, relating percentage and log of drug concentration in μM, as shown in Table 1. The observed results revealed thiosemicarbazones **22**, **23** and **24** as the most active compounds, with IC_{50} values of 20.7, 16.4 and 53.0 μM, respectively. The pentamidine was used as a positive control in the same assay conditions, with an IC_{50} of 4.8 μM.

2.2.2. Antileishmanial assays against L. amazonensis intracellular amastigotes

After demonstrating activity against extracellular promastigotes, the next step was to investigate the effect against intracellular amastigotes, the form of the parasite responsible for the mammalian infection. We determined that the most active compounds against promastigotes, **22** and **23**, were able to target the

Table 1
In vitro anti-leishmanial activity of new 6-X-piperonal thiosemicarbazones against promastigotes, intracellular amastigotes of *L. amazonensis* after 72 h of culture, and their cytotoxicity.

Compound	X	Promastigotes IC_{50} (μM)	Amastigotes[a] IC_{50} (μM)	Macrophages[b] LD_{50} (μM)	Selectivity index (SI)[c]
16	H	79.7 ± 5.5	nd[d]	nd	–
17	NO_2	270.8 ± 2.7	nd	nd	–
18	NH_2	118.8 ± 5.4	nd	nd	–
19	F	197.3 ± 4.9	nd	nd	–
20	Cl	243.9 ± 0.7	nd	nd	–
21	Br	202.3 ± 0.9	nd	nd	–
22	I	20.74 ± 0.5	22.0 ± 0.1	>125.0	>5.7
23	CN	16.4 ± 1.1	17.0 ± 1.1	>125.0	>7.4
24	OH	53 ± 5.1	nd	nd	–
26	$NHCOCH_2Cl$	256.3 ± 2.0	nd	nd	–
Pentamidine		4.8 ± 0.1	1.9 ± 0.1	8.5 ± 1.3	4.5

[a] Intracellular amastigotes.
[b] Murine peritoneal macrophages.
[c] SI = LD_{50}/IC_{50} intracellular amastigotes.
[d] nd: not determined.

Leishmania parasites inside of mouse peritoneal macrophages, without interfering with the viability of the host cells, with an IC_{50} of 22.0 and 17.0 μM, respectively. In similar conditions, pentamidine exhibited an IC_{50} of 1.9 μM.

These compounds were assayed against uninfected murine intraperitoneal macrophages to evaluate the cytotoxicity exhibiting LD_{50} > 125.0 μM (higher dose assayed) for both **22** and **23** and 8.5 μM of pentamidine.

Thus, the selectivity index (SI = LD_{50}/IC_{50} intracellular amastigotes) showed values of SI > 5.7 and SI > 7.3 for **22** and **23**, respectively, whereas SI = 4.5 for pentamidine, indicating the lower toxicity of the thiosemicarbazones. It is worth noting that due to experimental issues, it was not possible to evaluate concentrations higher than 125.0 μM. Therefore, the selectivity index of **22** and **23** may be even higher.

Samples of the amastigote-infected macrophages treated with thiosemicarbazones **22** and **23** and without treatment (negative control) were observed by microphotography and revealed that the parasites were killed but that the host cells remained unaffected (Fig. 1).

2.3. 2D-QSAR model

To understand the role of parameters involved in the anti-leishmanial activity presented by 6-X-piperonal-derived thiosemicarbazones, the electronic, steric and lipophilicity properties represented by polarizability (POLZ), superficial tension (ST), volume molar (VM), molar refractivity (MR) and log *P* descriptors (Table 2) were calculated. These parameters were all calculated with the ACDLabs software package (version 12.0), as Spessard [32] demonstrated its ability to simulate these parameters. From the results, the Hansh model was established [33,34]. The 2D-QSAR models were obtained via linear regression (LR) utilizing BuildQSAR software [35].

After analysing the generated models, it was possible to indicate a preliminary linear log *P* dependent model. This model of statistic parameters expressed the quality of the adjustment of the data in the model (r^2 = 0.80; F = 26.29) as well as the predictability (q^2 = 0.72), while considering compound **22** as an outlier and the CN moiety after hydrolysis at the pH of the performed assays ($CONH_2$), as shown in equation (1). However, when **22** and **24** were

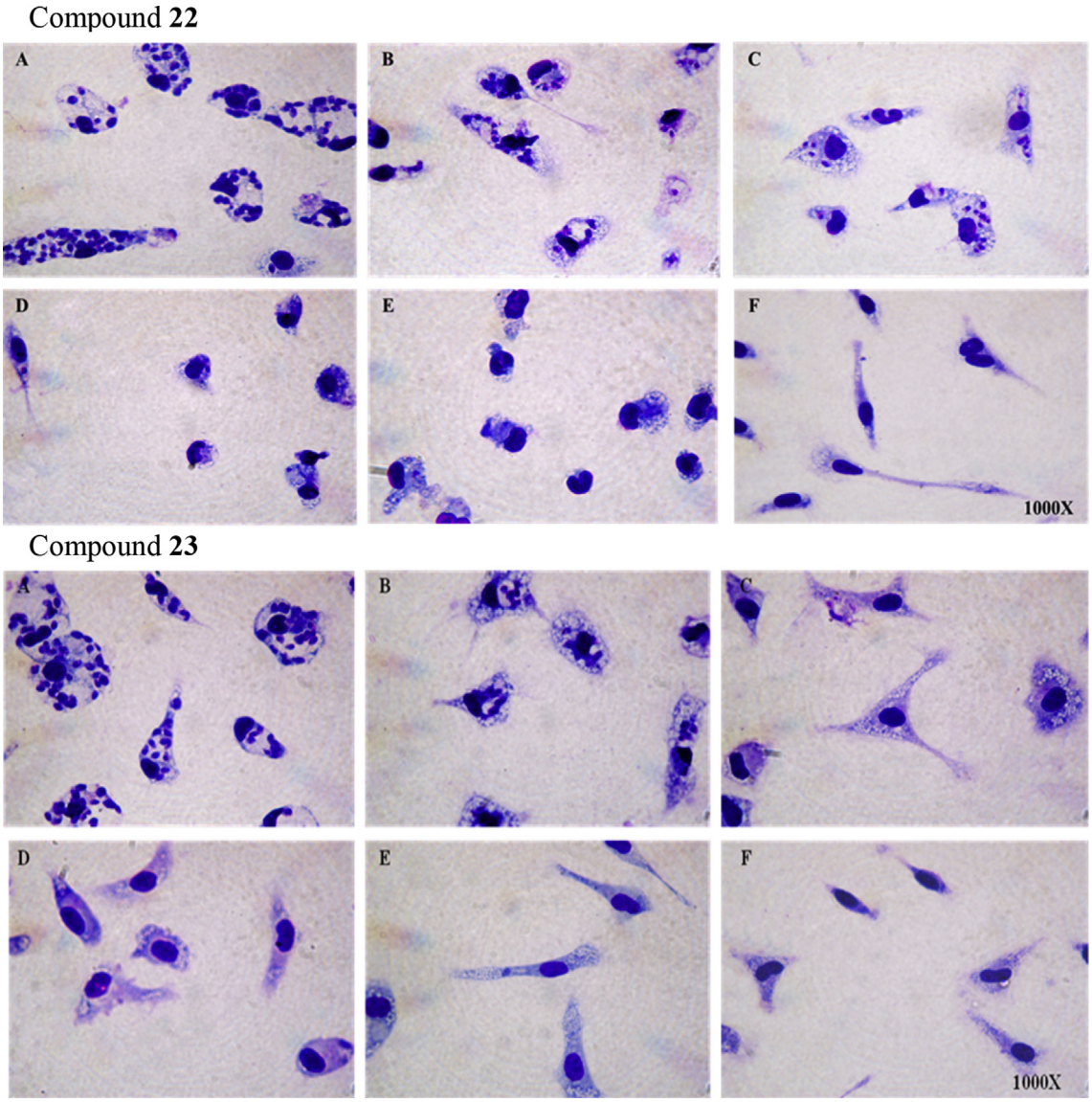

Fig. 1. Microphotographs of the *L. amazonensis*-infected macrophages treated with thiosemicarbazones **22** and **23** and those without treatment. After 72 h of culture, the slides were stained and parasites quantified by optical microscopy. (A) negative control; (B) 12.5 μM; (C) 25 μM; (D) 50 μM; (E) 100 μM; (F) no infected macrophages.

Table 2
Table of descriptors: log *P*, molecular refractivity (MR), molecular volume (MV), polarizability (POLZ), Hammett constant (σ_m), and Hansh constant (π_m).

Compound	log *P*[a]	MR[a]	MV[a]	POLZ[a]	σ_m[b]	π_m[c]
16	1.40	57.00	148.3	22.61	0	0
17	1.91	62.70	153.7	24.85	0.71	0.11
18	1.05	58.96	145.1	23.37	−0.16	−1.29
19	1.68	56.91	151.2	22.56	0.34	0.13
20	2.22	61.64	157.6	24.43	0.37	0.76
21	2.40	64.60	160.9	25.61	0.39	0.94
22	2.66	69.70	165.9	27.63	0.35	1.15
23	−1.08	64.42	158.5	25.30	0.28	0.0
24	1.54	57.90	145.6	22.95	0.12	−0.49
26	2.00	74.77	191.9	29.64	0.17	0.72

[a] ACDLabs software package version 12.0.
[b] Reference [34].
[c] Reference [36].

considered as outliers, the obtained model, also linear log *P* dependent, showed a higher quality setting of parameters than the 2D-QSAR model (Equation (2)).

$$\log A = +0.3483(\pm 0.1607)\log P + 1.5700(\pm 0.2822)$$
$$(n = 9;\ r^2 = 0.81;\ s = 0.200;\ F = 26.289;\ p = 0.0014;\ q^2 = 0.717) \quad (1)$$

$$\log A = +0.3525(\pm 0.1132)\log P + 1.6123(\pm 0.2017)$$
$$(n = 8;\ r^2 = 0.92;\ s = 0.136;\ F = 58.039;\ p = 0.0003;\ q^2 = 0.846) \quad (2)$$

The 2D-QSAR model demonstrates a linear relationship with log *P*, indicating the significance of lipophilicity.

2.4. Molecular docking

Compounds **22** and **23** are the most active compounds, with similar activities, but they also present very different ClogP values, which make it difficult a direct structure–activity relationship interpretation of the results. In a previous study from our group reporting the synthesis and activity of a series of thiosemicarbazones and semicarbazones against another trypanosomatid, *Trypanosoma cruzi*, it was shown that the most active compound was also able to significantly reduce the activity of NO synthase [16]. Based on these results, we decided to explore the corresponding enzyme in *Leishmania* with the molecular docking approach in order to obtain details at the molecular level of the ligands' interactions.

The best template that could be found with the Swiss-Model server was the 1TLL crystal structure from RCSB PDB, but the identity level between both sequences, 26.13%, was slightly below the homology modelling threshold [37]. The resulting model, however, presented an acceptable quality, with 93.2% of its residues in the favoured/allowed regions of the Ramachandran plot generated with the Rampage server [38], and a GMQE (Global Model Quality Estimation) value, which is a quality estimation expressed as a number between zero and one reflecting the expected accuracy of a model built with that alignment and its template [39], equal to 0.57.

This model was then used in a "blind" docking procedure with SwissDock, because NO synthase has many possible interaction sites for the ligands: NO synthase has at least binding sites for flavin adenine dinucleotide (FAD), flavin mononucleotide (FMN), heme, tetrahydrobiopterin (BH4) and calmodulin. Besides compounds **22** and **23A**, we also included in the docking procedure the less active compound, **17**, for a comparison.

The Gibbs free energy values calculated for the interaction (ΔG_{int}) between compounds **17**, **22**, **23A** and the LiNOS model were, respectively, −6.83 kJ/mol, −8.03 kJ/mol and −8.33 kJ/mol, in the same order of the observed activities. More importantly, no stable interaction modes could be found for compound **17** in the same binding site where compounds **22** and **23A** have their best ΔG_{int}, as can be seen in Fig. 2 and this could be the main reason for the low activity of this compound. In fact, as can be observed in Fig. 2B and C, although compounds **22** and **23A** have similar ΔG_{int}, they do not interact exactly in the same binding site. This is not surprising, because of the difference in properties of these compounds, as evidenced by the physicochemical descriptors presented in Table 2.

A superposition of the best binding modes of compounds **22** and **23A** with the template crystal structure (1TLL) (Fig. 3) reveals that compound **22** occupies partially the binding site containing a co-crystallized FMN molecule. Although compound **23A** does not occupy the same site, it is located in the gorge leading to the FMN binding site. So, we propose that both compounds interfere with the FMN binding, which is an essential prosthetic group of NO synthase.

3. Conclusion

In conclusion, a series of eleven 3,4-methylenedioxyde-6-X-benzaldehyde-thiosemicarbazones with various electronic features, ten of which are described for the first time, were prepared in good yields. Among all compounds tested against *L. amazonensis*, the 6-I and 6-CN substituted thiosemicarbazones showed significant antileishmanial activity and selectivity indices higher than pentamidine, from molecular docking can been observed both compounds interacting binding site FMI, important site of NO synthase. The results suggest that these compounds can be used as promising novel prototypes for drug development against leishmaniasis.

4. Experimental section

4.1. General methods

The melting points were recorded on a Mel-Temp II capillary meting point apparatus and are uncorrected. The IR spectra were recorded on a Bruker Vertex 70 spectrophotometer using potassium bromide tablets. ^1H and ^{13}C NMR spectra were obtained in Bruker NMR Ultrashield 400 MHz and 500 MHz spectrometers, with tetramethysilane as the internal reference and DMSO-d_6 as the solvent; the chemical shifts are reported in ppm. Mass spectrums were recorded using a Saturn GC–MS - CP-SIL8CB (30 m × 25 mm × 25 mm). Reactions were monitored by TLC on Merck silica gel 60 F254 aluminium sheets. TLC spots were visualised by inspection of the plates under UV light (254 and 365 mm). All commercial reagents were obtained from Aldrich or Merck Co. and used without any further purification.

4.1.1. Synthesis

*4.1.1.1. General procedure to synthesis of 3,4-methylenedioxyde-6-X-benzaldehyde-thiosemicarbazones (**16**–**26**).* To a solution of 3,4-methylenedioxyde-6-X-benzaldehyde (0.01 mol), previously crushed, in hot ethanol (30 mL) was added two drops of concentrated sulphuric acid and thiosemicarbazide (0.01 mol). The reaction mixture was stirred at 40 °C for 4 h, and monitored by TLC. The precipitate was filtered off and recrystallised from ethanol.

Fig. 2. Comparison of interaction modes obtained with the "blind" docking of SwissDock for selected compounds: (A) superposition of all clusters obtained for compound **17**; (B) best interaction mode for compound **22**; (C) best interaction mode for compound **23A**. Protein in cartoon representation; ligands in stick representation. Colour code: carbon, grey; oxygen, red; nitrogen, blue; hydrogen, white; sulphur, yellow; iodine, purple. Figure generated with Chimera 1.10.1 software. (For interpretation of the references to colour in this figure legend, the reader is referred to the web version of this article.)

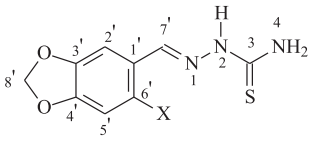

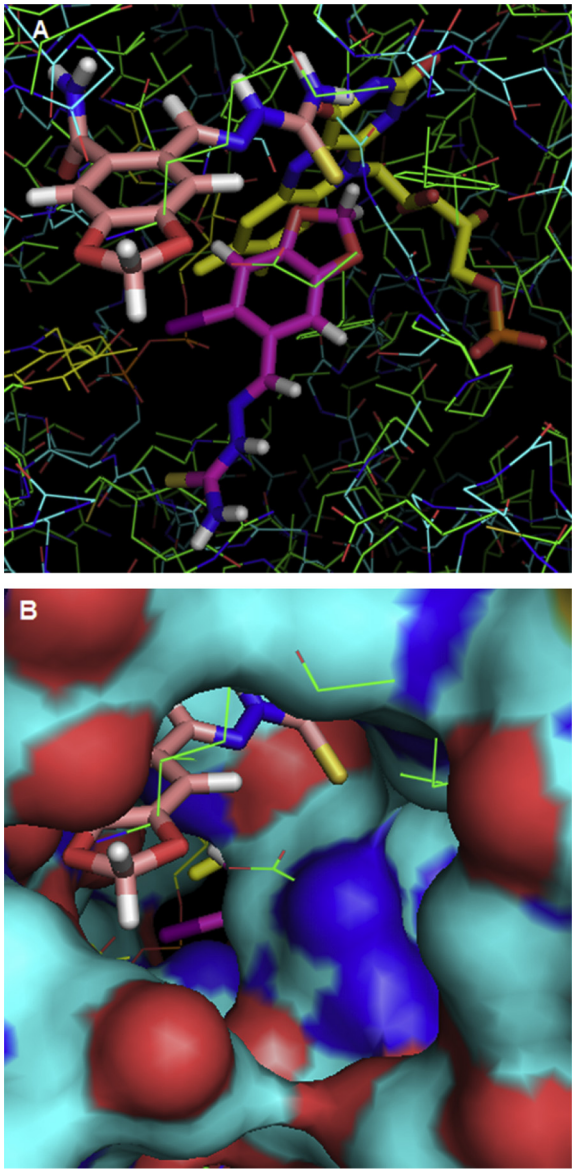

Fig. 3. (A) Superposition of the best binding modes of compounds **22** (carbon atoms in magenta, stick representation) and **23A** (carbon atoms in pink, stick representation) with the template crystal structure (PDB code 1TLL) (carbon atoms in green) containing a FMN molecule (carbon atoms in yellow, stick representation). In (B) it is presented the molecular surface of the parasite NO synthase showing the gorge leading to the FMN binding site. Colour code for the remaining atoms: oxygen, red; nitrogen, blue; hydrogen, white; sulphur, yellow; iodine, purple. Figures generated with PyMOL software. (For interpretation of the references to colour in this figure legend, the reader is referred to the web version of this article.)

*4.1.1.2. 3,4-Methylenedioxydebenzaldehyde-thiosemicarbazone (**16**).* White crystals; yield: 98%; m.p. 189 °C (literature 189 °C [40]). IR (KBr, cm^{-1}): 3464, 3323, 3134 (NH), 2966 (CH_2), 1541 (C=N), 1253 (C–O–C), 1082 (C=S). ^{1}H NMR (400 MHz, DMSO-d_6) δ: 11.34 (s, 1H, NH), 8.13, 8.05 (broad s, 2H, NH), 7.97 (s,1H, H7′), 7.64 (dd, $^3J_{H6'-H5'}$ = 8.5 Hz, $^4J_{H6'-H2'}$ = 1.8 Hz, 1H, H6′), 7.05 (d, $^4J_{H2'-H6'}$ = 1.8 Hz, 1H, H2′), 6.90 (d, $^3J_{H5'-H6'}$ = 8.5 Hz, 1H, H5′), 6.05 (s, 2H, H8′). ^{13}C NMR (DMSO-d_6, 100 MHz) δ: 178.3 (C3), 149.6 (C3′), 148.4 (C4′), 142.8 (C7′), 129.4 (C1′), 124.5 (C6′), 108.8 (C2′), 105.9 (C5′), 101.9 (C8′).

*4.1.1.3. 3,4-Methylenedioxyde-6-nitro-benzaldehyde-thiosemicarbazone (**17**).* Yellow crystals; yield: 96%; m.p. 238 °C. IR

(KBr, cm^{-1}): 3417, 3234 (NH_2), 3155 (NH), 2952(CH_2), 1541 (C=N), 1519, 1325 (NO_2), 1267 (C–O–C), 1033 (C=S). ^1H NMR (400 MHz, DMSO-d_6) δ: 11.65 (s, 1H, H2), 8.46 (s, 1H, H7′), 8.32 and 8.24 (broad s, 2H, H4 and H5), 7.99 (s, 1H, H5′), 7.54 (s, 1H, H2′), 6.25 (s, 2H, H8′). ^{13}C NMR (DMSO-d_6, 100 MHz) δ: 178.8 (C3), 152.2 (C3′), 149.0 (C6′), 143.6 (C4′), 137.9 (C7′), 126.1 (C1′), 106.3 (C2′), 105.1 (C5′), 104.1 (C8′). Anal. Calcd. for $C_9H_8N_4O_4S$: C, 40.30, H, 3.01, N, 20.89. Found: C, 40.15, H, 2.97, N, 20.97.

*4.1.1.4. 3,4-Methylenedioxyde-6-amino-benzaldehyde-thiosemicarbazone (**18**).* Greenish-yellow crystals; yield: 93%; m.p. 201 °C. IR (KBr, cm^{-1}): 3402, 3275 (NH_2), 3167 (NH), 2966 (CH_2), 1541 (C=N), 1259 (C–O–C), 1076 (C=S). ^1H NMR (400 MHz, DMSO-d_6) δ: 10.94 (s, 1H, H2), 8.06 (s, 1H, H7′), 7.96 and 7.72 (broad s, 2H, H4 and H5), 6.68 (s, 1H, H2′), 6.38 (s, 1H, H5′), 6.25 (broad s, 2H, H6′) 5.89 (s, 2H, H8′). ^{13}C NMR (DMSO-d_6, 100 MHz) δ: 176.7 (C3), 150.2 (C3′), 147.5 (C7′), 145.4 (C4′), 138.5 (C6′), 110.0 (C2′), 107.0 (C1′), 101.1 (C8′), 96.5 (C5′). Anal. Calcd. for $C_9H_{10}N_4O_2S$: C, 45.37, H, 4.23, N, 23.51. Found: C, 45.42, H, 4.19, N, 23.47.

*4.1.1.5. 3,4-Methylenedioxyde-6-fluoro-benzaldehyde-thiosemicarbazone (**19**).* White crystals; yield: 95%; m.p. 205 °C. IR (KBr, cm^{-1}): 3417, 3228 (NH_2), 3145 (NH), 2977 (CH_2), 1535 (C=N), 1325 (C–F), 1240 (C–O–C), 1097 (C=S). ^1H NMR (400 MHz, DMSO-d_6) δ: 11.50 (s, 1H, H2), 8.09 (broad s, 1H, H4), 8.02 (s, 1H, H7′), 7.77 (d, 1H $^4J_{H5'-H2'}$ = 1.5 Hz, H5′), 7.59 (d, 1H, $^4J_{H2'-H5'}$ = 1.5 Hz, H2′), 7.36 (broad s,1H, H5), 6.12 (s, 2H, H8′). ^{13}C NMR (DMSO-d_6, 100 MHz) δ: 177.7 (C3), 158.3 (C6′), 150.2 (C4′), 147.8 (C3′), 142.3 (C7′), 122.2 (C1′), 116.3 (C2′), 102.1 (C8′), 97.1 (C5′). Anal. Calcd. for $C_9H_8FN_3O_2S$: C, 44.81, H, 3.34, N, 17.42. Found: C, 44.87, H, 3.29, N, 17.51.

*4.1.1.6. 3,4-Methylenedioxyde-6-chloro-benzaldehyde-thiosemicarbazone (**20**).* Greenish crystals; yield: 98%; m.p. 208 °C. IR (KBr, cm^{-1}): 3477, 3332 (NH_2), 3143 (NH), 2970 (CH_2), 1539 (C=N), 1245 (C–O–C), 1089 (C=S), 667 (C–Cl). ^1H NMR (400 MHz, DMSO-d_6) δ: 11.51 (s, 1H, H2), 8.37 (s, 1H, H7′), 8.23 and 8.19 (broad s, 2H, H4 and H5), 7.92 (s, 1H, H5′), 7.10 (s, 1H, H2′), 6.12 (s, 2H, H8′). ^{13}C NMR (DMSO-d_6, 100 MHz) δ: 178.4 (C3), 1450.0 (C4′), 147.8 (C3′), 138.7 (C7′), 126.9 (C1′), 125.7 (C6′), 109.9 (C2′), 106.3 (C5′), 102.9 (C8′). Anal. Calcd. for $C_9H_8ClN_3O_2S$: C, 41.95, H, 3.13, N, 16.31. Found: C, 41.81, H, 3.07, N, 16.42.

*4.1.1.7. 3,4-Methylenedioxyde-6-bromo-benzaldehyde-thiosemicarbazone (**21**).* White crystals; yield: 97%; m.p. 216 °C. IR (KBr, cm^{-1}): 3477, 3323 (NH_2), 3151 (NH), 2972 (CH_2), 1535 (C=N), 1245 (C–O–C), 1093 (C=S), 568 (C–Br). ^1H NMR (400 MHz, DMSO-d_6) δ: 11.53 (s, 1H, H2′), 8.34 (s, 1H, H7′), 8.21 and 8.18 (broad s, 2H, H4 and H5), 7.91 (s, 1H, H5′), 7.22 (s, 1H, H2′), 6.12 (s, 2H, H8′). ^{13}C NMR (DMSO-d_6, 100 MHz) δ: 178.5 (C3), 150.2 (C4′), 148.3 (C3′), 141.2 (C7′), 127.2 (C1′), 116.1 (C6′), 112.8 (C2′), 106.9 (C5′), 102.9 (C8′). Anal. Calcd. for $C_9H_8BrN_3O_2S$: C, 35.78, H, 2.67, N, 13.91. Found: C, 35.82, H, 2.61, N, 14.02.

*4.1.1.8. 3,4-Methylenedioxyde-6-iodo-benzaldehyde-thiosemicarbazone (**22**).* White crystals; yield: 99%; m.p. 213 °C. IR (KBr, cm^{-1}): 3417, 3228 (NH_2), 3145 (NH), 2977 (CH_2), 1535 (C=N), 1240 (C–O–C), 1097 (C=S), 561 (C–I). ^1H NMR (400 MHz, DMSO-d_6) δ: 11.56 (s, 1H, H2), 8.25 (s, 1H, H7′), 8.19 and 8.15 (broad s, 2H, H4 and H5), 7.87 (s, 1H, H5′), 7.39 (s, 1H, H2′), 6.10 (s, 2H, H8′). ^{13}C NMR (DMSO-d_6, 100 MHz) δ: 178.3 (C3), 150.2 (C4′), 149.0 (C3′), 145.8 (C7′), 130.1 (C1′), 118.6 (C6′), 107.2 (C2′), 102.6 (C8′), 90.7 (C5′). Anal. Calcd. for $C_9H_8IN_3O_2S$: C, 30.96, H, 2.31, N, 12.04. Found: C, 30.90, H, 2.38, N, 12.11.

*4.1.1.9. 3,4-Methylenedioxyde-6-cyano-benzaldehyde-thiosemicarbazone (**23**).* White crystals; yield: 93%; m.p. 210 °C. IR (KBr, cm^{-1}): 3477, 3332 (NH_2), 3143 (NH); 2976 (CH_2), 2230 (C≡N), 1539 (C=N), 1240 (C–O–C), 1089 (C=S). ^1H NMR (400 MHz, DMSO-d_6) δ: 11.45 (s, 1H, H2), 8.35 (s, 1H, H7′), 8.21 and 8.17 (broad s, 2H, H4 and H5), 7.52 (s, 1H, H5′), 7.19 (s, 1H, H2′), 6.12 (s, 2H, H8′). ^{13}C NMR (DMSO-d_6, 100 MHz) δ: 178.9 (C3), 154.6 (C3′), 151.7 (C4′), 144.5 (C7′), 131.9 (C1′), 116.1 (C9′), 114.6 (C5′), 111.5 (C2′), 1085 (C6′), 101.6 (C8′). Anal. Calcd. for $C_{10}H_8N_4O_2S$: C, 48.38, H, 3.25, N, 22.57. Found: C, 48.42, H, 3.31, N, 22.64.

*4.1.1.10. 3,4-Methylenedioxyde-6-hydroxy-benzaldehyde-thiosemicarbazone (**24**).* White crystals; yield: 93%; m.p. 212 °C. IR (KBr, cm^{-1}): 3446, 3330 (NH_2), 3134 (NH), 2947 (CH_2), 2966 (O–H), 1541 (C=N), 1269 (C–O–C), 1064 (C=S). ^1H NMR (400 MHz, DMSO-d_6) δ: 11.25 (s,1H, H2), 9,84 (broad s,1H, H6′), 8.27 (s, 1H, H7′), 7.98 and 7.95 (broad s, 2H, H4 and H5), 7.55 (s,1H, H2′), 6.45 (s,1H, H5′), 5.96 (s, 2H, H8′). ^{13}C NMR (DMSO-d_6, 100 MHz) δ: 177.7 (C3), 153.2 (C6′), 150.1 (C4′), 141.3 (C3′), 140.0 (C7′), 113.3 (C1′), 105.0 (C2′), 101.7 (C8′), 98.0 (C5′). Anal. Calcd. for $C_9H_9N_3O_3S$: C, 45.18, H, 3.79, N, 17.56. Found: C, 45.23, H, 3.82, N, 17.66.

*4.1.1.11. 3,4-Methylenedioxyde-6-methoxy-benzaldehyde-thiosemicarbazone (**25**).* White crystals; yield: 91%; m.p. 207 °C. IR (KBr, cm^{-1}): 3446, 3359 (NH_2), 3174 (NH), 2976 (CH_2), 2929 (C–H), 1539 (C=N), 1244 (C–O), 1082 (C=S). ^1H NMR (400 MHz, DMSO-d_6) δ: 11.45 (s, 1H, H2), 8.22 (s, 1H, H7′), 8.05 and 7.98 (broad s, 2H, H4 and H5), 7.65 (s, 1H, H5′), 6.45 (s, 1H, H2′), 5.99 (s, 2H, H8′), 3.86 (s, 3H, H9′). ^{13}C NMR (DMSO-d_6, 100 MHz) δ: 177.5 (C3), 151.8 (C6′), 149.1 (C4′), 144.8 (C3′), 141.2 (C7′), 119.1 (C1′), 110.2 (C2′), 102.9 (C8′), 92.9 (C5′), 55.9 (C9′).

*4.1.1.12. 3,4-Methylenedioxyde-6-aminochloroacetyl-benzaldehyde-thiosemicarbazone (**26**).* White-Greenish crystals; yield: 95%; m.p. 257 °C. IR (KBr, cm^{-1}): 3473, 3352 (NH_2), 3168 (NH), 2974 (CH_2), 1652 (C=O), 1506 (C=N), 1238 (C–O–C), 1099 (C=S), 667 (C–Cl). ^1H NMR (400 MHz, DMSO-d_6) δ: 11.60 (broad s, 1H, H6′); 10,66 (s, 1H, H2); 8,38 (s, 1H, H5′); 8,12 (s, 1H, H7′); 7,99 e 7,72 (broad s, 2H, H4 and H5), 6.60 (s, 1H, H2′), 5.92 (s, 2H, H8′), 4.21 (s, 2H, H9′). ^{13}C NMR (DMSO-d_6, 100 MHz) δ: 178.1 (C3), 165.9 (C9′), 151.9 (C4′), 148.9 (C7′), 145.8 (C3′), 132.8 (C6′), 125.8 (C1′), 113.1 (C2′), 102.5 (C8′), 91.6 (C5′), 43.1 (C10′). Anal. Calcd. for $C_{11}H_{11}ClN_4O_3S$: C, 41.98, H, 3.52, N, 17.80. Found: C, 41.90, H, 3.48, N, 17.88.

4.2. Biological assays

4.2.1. Parasites

L. amazonensis (strain: MHOM/BR/77/LTB0016) was maintained as promastigotes at 26 °C in Schneider's insect medium (Sigma–Aldrich, St Louis, MO, USA) with 10% serum, 100 mg/mL streptomycin and 100 U/mL penicillin. Parasites were maintained until the 10th passage; subsequently, new cultures were obtained from infected animals. The Animal Ethics Committee of the Oswaldo Cruz Foundation (license number LW07/2010) approved this study.

4.2.2. Promastigote inhibition growth assay

Promastigotes of *L. amazonensis* (LTB0016, 1×10^6/mL) were incubated with thiosemicarbazones up to 400 μM for 72 h at 26 °C in Schneider's medium supplemented with 10% FBS, penicillin (100 UI/mL) and streptomycin (100 μg/mL). The assays were performed in triplicate in 96-well plates (Costar, New York, USA). The inhibition growth assay was evaluated by adding 22 μL of MTT (5 mg/mL, Sigma, Saint Louis, USA) per well. After 2 h, 80 μL of DMSO (Vetec, Rio de Janeiro, Brazil) was added to each well, and the optical density was measured at 570 nm using a spectrometer (Bio-Tek

Instruments, Winooski, USA). Alternatively, for samples where colour interfered with the spectrometer measurement, the parasites were quantified by light microscopy. The 50% inhibitory concentration (IC_{50}) was determined by logarithmic regression analysis in GraphPad Prism 5.0. All assays were performed in triplicate in three independent experiments. The final concentration of DMSO (Sigma) used to solve the thiosemicarbazones did not exceed 1% in the cultures.

4.2.3. Antiamastigote assay

To evaluate the activity against intracellular amastigotes, resident macrophages from BALB/c mice were obtained by peritoneal lavage with 5 mL of cold RPMI medium (Sigma). The cell suspension was adjusted to a concentration of 2×10^6/mL and plated in Lab-tek chambers (Nunc). After 1 h, the cultures were washed with phosphate-buffered saline (PBS) at 37 °C to remove non-adherent cells. The remaining cells were incubated at 37 °C/5% CO_2 with promastigotes of *L. amazonensis* at a ratio of 3:1. After 3 h, the chambers were washed again to remove free parasites. The monolayers were incubated with thiosemicarbazones up to 100 μM for 72 h at 37 °C/5% CO_2. The antiamastigote activity was evaluated microscopically after staining the chambers with the Instant Prov haematological dye system (Newprov, Curitiba, Brazil); at least 200 macrophages were counted per sample. The results are expressed as the infection index (IF) using the following formula: IF = % infected cells × number of amastigotes/total macrophages. The calculation of the IC_{50} was performed by logarithmic regression, and the statistical analysis was performed using Student's t test in GraphPad Prism 5.0 software.

4.2.4. Cytotoxicity

BALB/c mice macrophages were obtained by peritoneal lavage with cold RPMI medium (Sigma®). The macrophages at 2×10^6 cells/well in RPMI culture medium (pH 7.2, supplemented with 10% foetal bovine serum) were incubated with prototypes (0–125 μM) for 72 h at 37 °C under 5% CO_2 in 96-well plates. After removing the supernatant, viable cells were quantified by adding Resazurin solution in phosphate buffer saline. The fluorescence was measured using a Spectra Max M2 spectrofluorometer (Molecular Devices, Silicon Valley, USA) at excitation and emission wavelengths of 560 nm and 590 nm, respectively. The percentage of viable cells was calculated relative to the control cells. The tests were carried out in triplicate.

4.2.5. Molecular docking

There is no crystallographic structure available for the NO synthase from any Leishmania species, so it was necessary the construction of a homology model for the enzyme. Unfortunately, there is a paucity of sequencing data for *L. amazonensis* proteins in the literature, so it was necessary to select the NO synthase sequence from another Leishmania species to apply the homology modelling procedure. In fact, there is only one NO synthase sequence from a Leishmania species available in the UniProtKB/Swiss-Prot database, that from *Leishmania infantum* (code A4HYH5), which is a member of the same subgenus of *L. amazonensis*, Leishmania (the more accurate definition of this species is *Leishmania Leishmania amazonensis*). The *L. infantum* NO synthase (LiNOS) model was constructed with the automated mode of the Swiss-Model protein structure homology-modelling server [39].

The ligands' structures were constructed and energy-minimized with the PM6 method [41] available in the Spartan'14 software (Wavefunction, Inc.). For compound **23**, we modelled its hydrolysis product, were the cyano group was replaced by an amide group, defined as compound **23A**. Docking studies were implemented with the SwissDock server [42]. SwissDock is based on the docking software EADock DSS [43], whose algorithm consists of the generation of many binding modes either in a box (local docking) or in the vicinity of all target cavities (blind docking), followed by the estimation of their energies on a grid with CHARMM [44]. The binding modes with the most favourable energies are evaluated with the FACTS solvation model [45], and then clustered.

Acknowledgements

The authors thank CNPq (Conselho Nacional de Desenvolvimento Científico e Tecnológico) (3808181/2011-5), CAPES (Coordenação de Aperfeiçoamento de Pessoal de Nível Superior) (E-26/110.590/2012), and FAPERJ (Fundação de Apoio à Pesquisa do Estado do Rio de Janeiro) for financial support and fellowships received.

Appendix A. Supplementary data

Supplementary data related to this article can be found at http://dx.doi.org/10.1016/j.ejmech.2015.09.009.

References

[1] S. Singh, R. Sivakumar, Challenges and new discoveries in the treatment of leishmaniasis, J. Infect. Chemother. 10 (2004) 307–315.
[2] H.W. Murray, J.D. Berman, C.R. Davies, Advances in leishmaniasis, Lancet 366 (2005) 1561–1577.
[3] WHO, Report of a Meeting of the WHO Expert Committee on the Control of the Leishmaniases, Geneva, 2010.
[4] (a) D. Plano, Y. Baquedano, D. Moreno-Mateos, M. Font, A. Jiménez-Ruiz, J.A. Palop, C. Sanmartín, Selenocyanates and diselenides: a new class of potente antileishmanial agents, Eur. J. Med. Chem. 46 (2011) 3315–3323; (b) R.F. Rodrigues, D. Castro-Pinto, A. Echevarria, C.M. Reis, C.N. Del Cistia, C.M.R. Sant'Anna, F. Teixeira, H. Castro, M. Canto-Cavalheiro, L.L. Leon, A. Tomás, Investigation of trypanothione reductase inhibitory activity by 1,3,4-thiadiazolium-2-aminide derivatives and molecular docking studies, Bioorg. Med. Chem. 20 (2012) 1760–1766.
[5] T.K. Jha, Drug unresponsiveness & combination therapy for kala-azar, Indian J. Med. Res. 123 (2006) 389–398.
[6] P. Rudrapaul, I.S. Sarma, N. Das, U.C. De, S. Bhattacharjee, B. Dinda, New flavonol methyl ether from the leaves of *Vitex peduncularis* exhibits potential inhibitory activity against *Leishmania donovani* through activation of iNOS expression, Eur. J. Med. Chem. 87 (2014) 328–335.
[7] T.T. Guimarães, M.C.F.R. Pinto, J.S. Lanza, M.N. Melo, R.L. Monte-Neto, I.M.M. Melo, E.B.T. Diogo, V.F. Ferreira, C.A. Camara, W.O. Valença, R.N. Oliveira, F. Frézard, E.N. Silva-Júnior, Potent naphthoquinones against antimony-sensitive and -resistant Leishmania parasites: synthesis of novel α- and nor-α-lapachone-based 1,2,3-triazoles by copper-catalyzed azide-alkyne cycloaddition, Eur. J. Med. Chem. 63 (2013) 523–530.
[8] S. Oh, S. Kim, S. Kong, G. Yang, N. Lee, D. Han, J. Goo, J.L. Siqueira-Neto, L.H. Freitas-Junior, R. Song, Synthesis and biological evaluation of 2,3-dihydroimidazo[1,2-a]benzimidazole derivatives against *Leishmania donovani* and *Trypanosoma cruzi*, Eur. J. Med. Chem. 84 (2014) 395–403.
[9] A.Y. Lukmantara, D.S. Kalinowski, N. Kumar, D.R. Richardson, Synthesis and biological evaluation of substituted 2-benzoylpyridine thiosemicarbazones: novel structure-activity relationships underpinning their anti-proliferative and chelation efficacy, Bioorg. Med. Chem. Lett. 23 (2013) 967–974.
[10] J.A. Lessa, I.C. Mendes, P.R.O. da Silva, M.A. Soares, R.G. dos Santos, N.L. Speziali, N.C. Romeiro, E.J. Barreiro, H. Beraldo, 2-Acetylpyridine thiosemicarbazones: cytotoxic activity in nanomolar doses against malignant gliomas, Eur. J. Med. Chem. 45 (2010) 5671–5677.
[11] F.R. Pavan, P.I.S. Maia, S.R.A. Leite, V.M. Daflon, A.A. Batista, D.N. Sato, S.G. Franzblau, C.Q.F. Leite, Thiosemicarbazones, semicarbazones, dithiocarbazates and hydrazide/hydrazones: anti-Mycobacterium tuberculosis activity and cytotoxicity, Eur. J. Med. Chem. 45 (2010) 1898–1905.
[12] A.K. Halve, B. Bhashkar, V. Sharma, R. Bhadauria, A. Kankoriya, A. Soni, K. Tiwari, Synthesis and in vitro antimicrobial studies of some new 3- [phenyldiazenyl]benzaldehyde *N*-phenylthiosemicarbazones, J. Enzym. Inhib. Med. Chem. 23 (2008) 77–81.
[13] R.J. Glisoni, M.L. Cuestas, V.L. Mathet, J.R. Oubiña, A.G. Moglioni, A. Sosnik, Antiviral activity against the hepatitis C virus (HCV) of 1-indanone thiosemicarbazones and their inclusion complexes with hydroxypropyl-β-cyclodextrin, Eur. J. Pharm. Sci. 47 (2012) 596–603.
[14] M.E. Caputto, L.E. Fabian, D. Benítez, A. Merlino, N. Ríos, H. Cerecetto, G.Y. Moltrasio, A.G. Moglione, M. Gonzáles, L.M. Finkielstein, Thiosemicarbazones derived from 1-indanones as new anti-*Trypanosoma cruzi* agents, Bioorg. Med. Chem. 19 (2011) 6818–6826.
[15] J.P. Mallari, W.A. Guiguemde, R.K. Guy, Antimalarial activity of

thiosemicarbazones and purine derived nitriles, Bioorg. Med. Chem. Lett. 19 (2009) 3546–3549.
[16] R.O.A. Soares, A. Echevarria, M.S.S. Bellieny, R.T. Pinho, R.M.M. de Leo, W.S. Seguins, G.M. Machado, M.M. Canto-Cavalheiro, L.L. Leon, Evaluation of thiosemicarbazones and semicarbazones as potential agents anti-Trypanosoma cruzi, Exp. Parasitol. 129 (2011) 381–387.
[17] A. Moreno-Rodríguez, P.M. Salazer-Schettino, J.L. Bautista, F. Hernández-Luis, H. Torrens, Y. Guevara-Gomez, S. Pina-Canseco, M.B. Torres, M. Cabrera-Bravo, C.M. Martinez, E. Perez-Campos, In vitro antiparasitic activity of new thiosemicarbazones in strains of *Trypanosoma cruzi*, Eur. J. Med. Chem. 87 (2014) 23–29.
[18] C.D. Duarte, J.L.M. Tributino, D.I. Lacerda, M.V. Martins, M.S. Alexandre-Moreira, F. Dutra, E.J.H. Bechara, F.S. de Paula, M.O.F. Goulart, J. Ferreira, J.B. Calixto, M.P. Nunes, A.L. Bertho, A.L.P. Miranda, E.J. Barreiro, C.A.M. Fraga, Synthesis, pharmacological evaluation and electrochemical studies of novel 6-nitro-3,4-methylenedioxyphenyl-N-acylhydrazone derivatives, Bioorg. Med. Chem. 15 (2007) 2421–2433.
[19] W.O. Lin, E.S. Coutinho, 8,9-Methylenedioxy-3,4-dihydro-1,4,5- benzotriazocin-2(1H)-ones, Monatsh. Chem. 11 (1983) 1231–1235.
[20] T. Furuya, J.E.M.N. Klein, T. Ritter, C-F bond formation for the synthesis of aryl fluorides, Synthesis 11 (2010) 1804–1821.
[21] A.A. Moraes, R. Braz-Filho, S.V. Fraiz, Synthesis of three natural 1,3- diarylpropanes: two revised structures, Phytochem 28 (1988) 239–242.
[22] S.N. Aslam, P.C. Stevenson, S.J. Phythian, N.C. Veitch, D.R. Hall, Synthesis of cicerfuran, an antifungal benzofuran, and some related analogues, Tetrahedron 62 (2006) 4214–4226.
[23] G.F. Mendonça, M.C.S. Mattos, Uma metodologia simples e eficiente para a cloração de compostos aromáticos ativados utilizando o ácido tricloro-isocianúrico, Quím. Nova 31 (2008) 798–801.
[24] M. Luo, H.Z. Ma, Q.D. Su, Q.R. Li, Synthesis and crystal structure of 6-bromo-piperonal-dimethyl-acetal, Chin. J. Struct. Chem. 21 (2002) 538–540.
[25] T.N. LE, C. Won-Jea, Total synthesis of oxyfagaronine, phenolic benzo- [c] phenanthridine and general synthetic way of 2,3,7,8-and 2,3,8,9- tetrasubstituted benzo[c]phenanthridine alkaloids, Chem. Pharm. Bull. 54 (2006) 476–480.
[26] T. Shigemitsu, H. Abe, Y. Takeuchi, T. Harayama, Intramolecular biaryl coupling reaction of benzyl benzoate and phenyl benzoate derivatives, and its applications to the formal synthesis of (-)-steganone, Tetrahedron 63 (2007) 396–408.
[27] D. Crich, V. Krishnamurthy, Radical dearomatization of benzene leading to phenanthridine and phenantridinone derivatives related to (±)-pancrastistatin, Tetrahedron 62 (2006) 6830–6840.
[28] P.R. Tenório, A.J.S. Góes, A.R. Faria, A.J. Alves, T.M. Aquino, Tiossemicarbazonas: métodos de obtenção, aplicações sintética e importância biológica, Quim. Nova 28 (2005) 1030–1037.
[29] H. Beraldo, A.M. Barreto, R.P. Vieira, A.P. Rebolledo, N.L. Spezialib, C.B. Pinheiro, G. Chapuisc, Structural studies and spectral characteristics of 4-benzoylpyridine thiosemicarbazone and N(4′)-phenyl-4-benzoylpyridine thiosemicarbazone, J. Mol. Struct. 6454 (2003) 213–220.
[30] J.B.P. Silva, F. Hallwass, A.G. da Silva, D.R. Moreira, M.N. Ramos, J.W.P. Espindola, A.D.T. Oliveira, D.J. Brondani, A.C.L. Leite, K.M. Merz Jr., Intermolecular interaction of thiosemicarbazone derivatives to solvents and a potential *Aedes aegypti* target, J. Mol. Struct. 1093 (2015) 219–227.
[31] R.J. Soares-Bezerra, L.L. Leon, A. Echevarria, C.M. Reis, L. Gomes-Silva, C.G. Agostinho, M.M. Canto-Cavalheiro, M. Genestra, In vitro evaluation of 4-phenyl-5-(4-X-phenyl)-1,3,4-thiadiazolium-2-phenylaminide chlorides and 3-[N-4-X-phenyl]-1,2,3-oxadiazolium-5-olate derivatives on nitric oxide synthase and arginase of *Leishmania amazonensis*, Bioorg. Med. Chem. 135 (2013) 50–54.
[32] G.O. Spessard, ACD labs/log P dB 3.5 and ChemSketch 3.5, J. Chem. Inf. Comput. Sci. 38 (1998) 1250–1253.
[33] H. Kubinyi, QSAR and 3D QSAR in drug design, Part 2: applications and problems, Res. Focus 2 (1997) 457–467.
[34] C. Hansch, A. Leo, R.W. Taft, A survey of Hammett substituent constants and resonance and field parameters, Chem. Rev. 91 (1991) 165–195.
[35] D.D. Oliveira, A.C. Gaudio, BuildQSAR: a new computer program for QSAR analysis, Quant. Sctruct.-Act. Relat. 19 (2000) 599–601.
[36] T. Fujita, J. Iwasa, C. Hansch, A new substituent constant, π, derived from partition coefficients, J. Am. Chem. Soc. 86 (1964) 5175–5180.
[37] C. Sander, R. Schneider, Database of homology-derived protein structures and the structural meaning of sequence alignment, Proteins 9 (1991) 56–68.
[38] S.C. Lovell, I.W. Davis, W.B. Arendall III, P.I.W. de Bakker, J.M. Word, M.G. Prisant, J.S. Richardson, D.C. Richardson, Structure validation by calpha geometry: phi,psi and C beta deviation, Proteins Struct. Funct. Genet. 50 (2002) 437–450.
[39] M. Biasini, S. Bienert, A. Waterhouse, K. Arnold, G. Studer, T. Schmidt, F. Kiefer, T.G. Cassarino, M. Bertoni, L. Bordoli, T. Schwede, SWISS-MODEL: modelling protein tertiary and quaternary structure using evolutionary information, Nucleic Acids Res. 42 (2014) W252–W258.
[40] F. Beckford, J. Thessing, M. Shaloski Jr., P. Canisius Mbarushimana, A. Brock, J. Didion, J. Woods, A. Gonsalez-Sarrías, N.P. Seeram, Synthesis and characterization of mixed-ligand diimine-piperonal thiosemicarbazone complexes of ruthenium (II): biophysical investigations and biological evaluation as anticancer and antibacterial agents, J. Mol. Struct. 992 (2011) 39–47.
[41] J.J.P. Stewart, Optimization of parameters for semiempirical methods V: modification of NDDO approximations and application to 70 elements, J. Mol. Model 13 (2007) 1172–1213.
[42] A. Grosdidier, V. Zoete, O. Michielin, SwissDock, a protein-small molecule docking web service based on EADock DSS, Nucleic Acids Res. 39 (2011) W270–W277.
[43] A. Grosdidier, V. Zoete, O. Michielin, EADock: docking of small molecules into protein active sites with a multiobjective evolutionary optimization, Proteins Struct. Funct. Genet. 67 (2007) 1010–1025.
[44] B.R. Brooks, C.L. Brooks, A.D. Mackerell, L. Nilsson, R.L. Petrella, B. Roux, Y. Won, G. Archontis, C. Bartels, S. Boresch, A. Caflisch, L. Caves, Q. Cui, A.R. Dinner, M. Feig, S. Fischer, J. Gao, M. Hodoscek, W. Im, K. Kuczera, T. Lazaridis, J. Ma, V. Ovchinnikov, E. Paci, R.W. Pastor, C.B. Post, J.Z. Pu, M. Schaefer, B. Tidor, R.M. Venable, H.L. Woodcock, X. Wu, W. Yang, D.M. York, M. Karplus, CHARMM: the biomolecular simulation program, J. Comput. Chem. 30 (2009) 1545–1614.
[45] U. Haberthür, A. Caflisch, FACTS: fast analytical continuum treatment of solvation, J. Comput. Chem. 29 (2008) 701–715.